JUNB/AP-1 controls IFN-γ during inflammatory liver disease

Martin K. Thomsen,[1] Latifa Bakiri,[1] Sebastian C. Hasenfuss,[1] Rainer Hamacher,[1] Lola Martinez,[2] and Erwin F. Wagner[1]

[1]F-BBVA Cancer Cell Biology Programme and [2]Flow Cytometry Core Unit, National Cancer Research Centre (CNIO), Madrid, Spain.

Understanding the molecular pathogenesis of inflammatory liver disease is essential to design efficient therapeutic approaches. In hepatocytes, the dimeric transcription factor c-JUN/AP-1 is a major mediator of cell survival during hepatitis, although functions for other JUN proteins in liver disease are less defined. Here, we found that JUNB was specifically expressed in human and murine immune cells during acute liver injury. We analyzed the molecular function of JUNB in experimental models of hepatitis, including administration of concanavalin A (ConA) or α-galactosyl-ceramide, which induce liver inflammation and injury. Mice specifically lacking JUNB in hepatocytes displayed a mild increase in ConA-induced liver damage. However, targeted deletion of *Junb* in immune cells and hepatocytes protected against hepatitis in experimental models that involved NK/NKT cells. The absence of JUNB in immune cells decreased IFN-γ expression and secretion from NK and NKT cells, leading to reduced STAT1 pathway activation. Systemic IFN-γ treatment or adenovirus-based IRF1 delivery to *Junb*-deficient mice restored hepatotoxicity, and we demonstrate that *Ifng* is a direct transcriptional target of JUNB. These findings demonstrate that JUNB/AP-1 promotes cell death during acute hepatitis by regulating IFN-γ production in NK and NKT cells and thus functionally antagonizes the hepatoprotective function of c-JUN/AP-1 in hepatocytes.

Introduction

Inflammation of the liver (hepatitis) is mostly triggered by viral infections. Intoxications (notably alcohol), autoimmune diseases, metabolic disorders, fatty liver disease, and hereditary disorders are also important contributors to hepatitis and liver cancer development (1). Acute hepatitis is characterized by a strong innate inflammation, which induces hepatocyte cell death and can lead to liver failure (2, 3). Chronic, low-grade liver inflammation often progresses to fibrosis and cirrhosis, with permanent loss of organ function. Hepatitis is a strong risk factor for hepatocellular carcinoma development due to increased mutagenic reactive oxygen species and compensatory proliferation (3–5). Therefore, the hepatic innate immune responses have to be tightly balanced during acute hepatitis to ensure viral clearance without causing fatal liver damage or persisting low-grade inflammation.

IFNs are pleiotropic cytokines that play important roles during innate and adaptive immune response in the defense against viral and bacterial infections as well as in tumor surveillance (6). IFNs constitute the first line of response to viral infection. IFN-α and IFN-β are the best characterized type I IFNs, their expression is triggered by viral infections, and they in turn induce a number of antiviral gene products (7). The therapeutical potential of type I IFNs was assessed decades ago, and IFN-α is part of the standard therapeutic regiment for chronic viral hepatitis C infection (6, 8). IFN-γ, or type II IFN, is similarly induced by several pathogens, including viruses, but is also a key protein regulating T cell differentiation, activation, and homeostasis and an important activator of macrophages (9). IFN-γ is produced predominantly by NK and NKT cells as part of the innate immune response and by CD4 Th1 and CD8 T lymphocyte effector T cells during the adaptive immune response (10). Studies using mouse models indicated that IFN-γ and NKT cells participate in viral clearance, thereby preventing progression to chronic hepatitis (11, 12). However, the beneficial potential of IFN-γ administration to hepatitis-infected patients is still uncertain (13). IFN-γ activates the STAT1 pathway in hepatocytes and induces cell death, which can result in liver failure (14). Therefore, IFN-γ can be considered to be a double-edged sword during hepatitis, as it is crucial for viral defense but can also lead to liver damage. Defining the cellular and molecular signals controlling IFN-γ production during hepatitis is therefore of particular relevance to understanding the complex function of this cytokine and developing therapeutic approaches.

Activator protein 1 (AP-1) represents a family of dimeric transcription factors composed of JUN, Fos, and ATF proteins, which are central to several biological processes from embryonic development to various diseases (15). In particular, AP-1 has been shown to regulate the expression of several cytokines in a tissue/cell-specific manner (16). For instance, during in vitro T cell differentiation, JUN-containing dimers regulate *IL2*, *IL4*, and *IFNG* (17–21), whereas JUN proteins control skin inflammation in vivo by affecting *IL6* and *GMCSF* expression and TNF-α shedding in keratinocytes (22, 23). It is therefore likely that AP-1 transcription factors contribute to the inflammatory process during acute hepatitis. JUN proteins are very similar structurally, and members of the AP-1 transcription family can have specific or redundant functions (24). We have previously shown that c-JUN/AP-1 is necessary for the survival of hepatocytes during acute hepatitis. Surprisingly, c-JUN does not seem critical for immune response in this setting (25).

Here, we show that JUNB is strongly expressed in a subset of immune cells from liver samples from humans and mice with hepatitis. Using loss-of-function mouse models for JUNB, we unravel a novel function for JUNB/AP-1 in regulating the expression of *Ifng* in NK and NKT cells, thereby modulating acute liver damage and counteracting the protective function of c-JUN in hepatocytes.
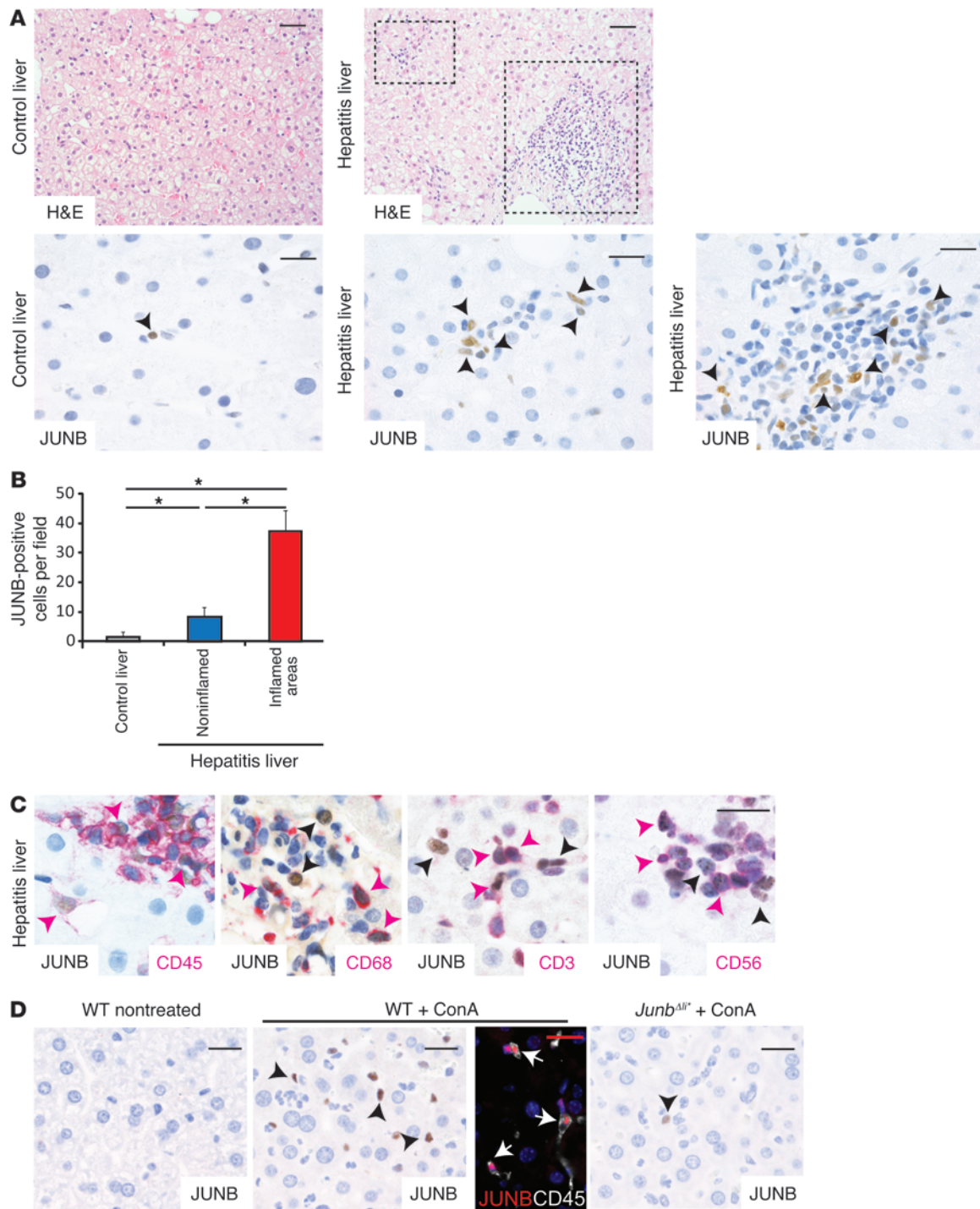
Figure 1
JUNB expression in immune cells from livers of patients with hepatitis. (**A**) Liver sections from healthy patients or patients with hepatitis were stained with H&E (scale bar: 50 μm) or with an antibody against JUNB (brown). Insets show representative inflamed areas. Black arrowheads indicate JUNB-positive cells (*n* = 5). Representative areas are shown. (**B**) Quantification of JUNB-positive cells in liver sections from healthy patients and those with hepatitis (*n* = 5, *P < 0.05). (**C**) Hepatitis samples were stained for JUNB (brown) and with a marker for immune cells (CD45), monocytes/macrophages (CD68), T cells (CD3), or NK and NKT cells (CD56) (red). JUNB-single positive cells are indicated with black arrowheads and double-positive cells are indicated with pink arrowheads. (**D**) Liver sections from wild type-mice treated or untreated with ConA for 2 hours and from ConA-treated *Junb*^Δli* mice were stained for JUNB (brown). Black arrowheads indicate JUNB-positive cells. Immune-fluorescence costaining of livers from ConA-treated mice for JunB (red) and CD45 (white). White arrows indicate double-positive cells. Scale bar: 20 μm. One representative experiment is shown (*n* > 5).
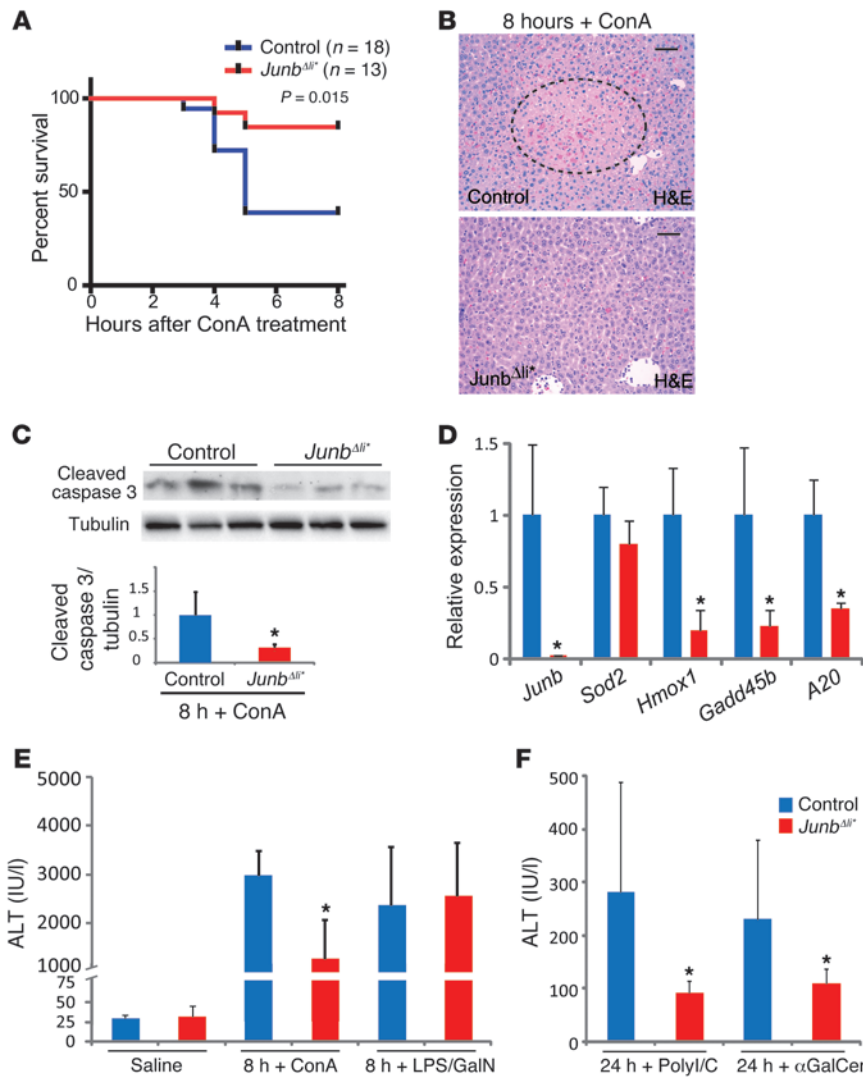
Figure 2
Junb$^{\Delta li*}$ mice are protected from liver damage upon ConA, αGalCer, and poly-I/C treatment. (**A**) Survival of control and *Junb*$^{\Delta li*}$ mice after ConA injection (25 mg/kg, Kaplan-Meier curve). (**B**) H&E staining of liver sections 8 hours after ConA treatment. The dotted line marks an area of liver damage. One representative experiment is shown ($n > 10$). Scale bar: 50 μm. (**C**) Western blot for cleaved caspase-3 and quantification relative to tubulin ($n = 5$; *$P < 0.05$). (**D**) qRT-PCR for stress-related genes 8 hours after ConA treatment ($n > 5$; *$P < 0.05$). Serum ALT levels (**E**) 8 or (**F**) 24 hours after injection of saline, ConA, LPS/GalN, αGalCer, or poly-I/C, as indicated ($n = 8$–12 mice per group; *$P < 0.05$).

and NKT cells are also essential (26–30). In nontreated wild-type mice, JUNB expression was not detectable in the liver by immunohistochemistry (IHC). However, 2 hours after ConA injection, JUNB was expressed strongly in nonparenchymal liver cells. Costaining with CD45 revealed that, similar to that in human hepatitis, JUNB-positive cells were also CD45 positive (Figure 1D). The specificity of the JUNB staining was confirmed using *Junb*$^{\Delta li*}$ mice (*Junb*$^{fl/fl}$; *MxCre*$^{T/+}$ mice), which lack JUNB in all liver cells (Figure 1D). Furthermore, flow cytometry analysis confirmed that upon ConA treatment, JUNB was expressed in a subset of T, Kupffer, NK, and NKT cells and that *Junb*$^{\Delta li*}$ mice had decreased JUNB expression in all cell types (Supplemental Figure 1, A and B; supplemental material available online with this article; doi:10.1172/JCI70405DS1). Importantly, the overall distribution of the different immune cells was not different between control and *Junb*$^{\Delta li*}$ mice, indicating that loss of JUNB did not impact on immune cell numbers (Supplemental Figure 1C). Finally, a similar increase of JUNB-positive immune cells was observed in 3 additional models of hepatitis: LPS/D-galactosamine (LPS/GalN), polyinosinic-polycytidylic acid (poly-I/C), and α-galactosyl-ceramide (αGalCer) administration (Supplemental Figure 1D). Collectively, our data indicate that JUNB is strongly expressed in immune cells of the liver during human and murine hepatitis, particularly in T, Kupffer, NK, and NKT cells.

Loss of JUNB in immune cells decreases liver damage in hepatitis mouse models involving NK/NKT cells. To investigate the functional relevance of JUNB in hepatitis, wild-type and *Junb*-deficient mice were treated with ConA and followed over 8 hours. Strikingly, *Junb*$^{\Delta li*}$ mice displayed increased survival rate (Figure 2A), which was also reflected by smaller necrotic areas observed by liver histology (Figure 2B) and by decreased cleaved caspase-3 protein (Figure 2C) and decreased *Hmox1*, *Gadd45b*, and *A20* mRNA (Figure 2D) in *Junb*$^{\Delta li*}$ livers. Serum alanine aminotransferase (ALT), a marker for liver damage, was also decreased in *Junb*$^{\Delta li*}$ mice (Figure 2E). Therefore, *Junb*$^{\Delta li*}$ mice are protected from liver damage and lethality induced by ConA treatment. We next used *Junb*$^{\Delta li}$

Results

JUNB is upregulated in human and mouse liver hepatitis. Expression of JUNB was assessed on paraffin sections of liver needle biopsies from patients with hepatitis and compared to nonhepatitis samples. Very few JUNB-positive cells were observed in healthy livers compared with those in hepatitis samples (Figure 1A). Quantification confirmed the increase of JUNB-positive cells, which was more pronounced in the inflamed areas, in liver samples from patients with hepatitis (Figure 1, A and B). CD45 staining indicated that all JUNB-positive cells were immune cells and not hepatocytes (Figure 1C). In combination with the JUNB antibody, we next used CD68, a marker for monocytes; CD3, a marker for T cells; and CD56, a cell surface marker for NK and NKT cells. Double-positive cells, likely JUNB-expressing Kupffer, T, NK, and NKT cells, were found in liver samples from patients with hepatitis, in particular, in the inflamed areas (Figure 1C). This analysis revealed that JUNB is expressed in immune cells of the liver and strongly increased during hepatitis.

JUNB expression was next analyzed in experimental models of hepatitis. In mice, concanavalin A (ConA) injection is a paradigm for T cell–dependent hepatitis, although macrophages and NK
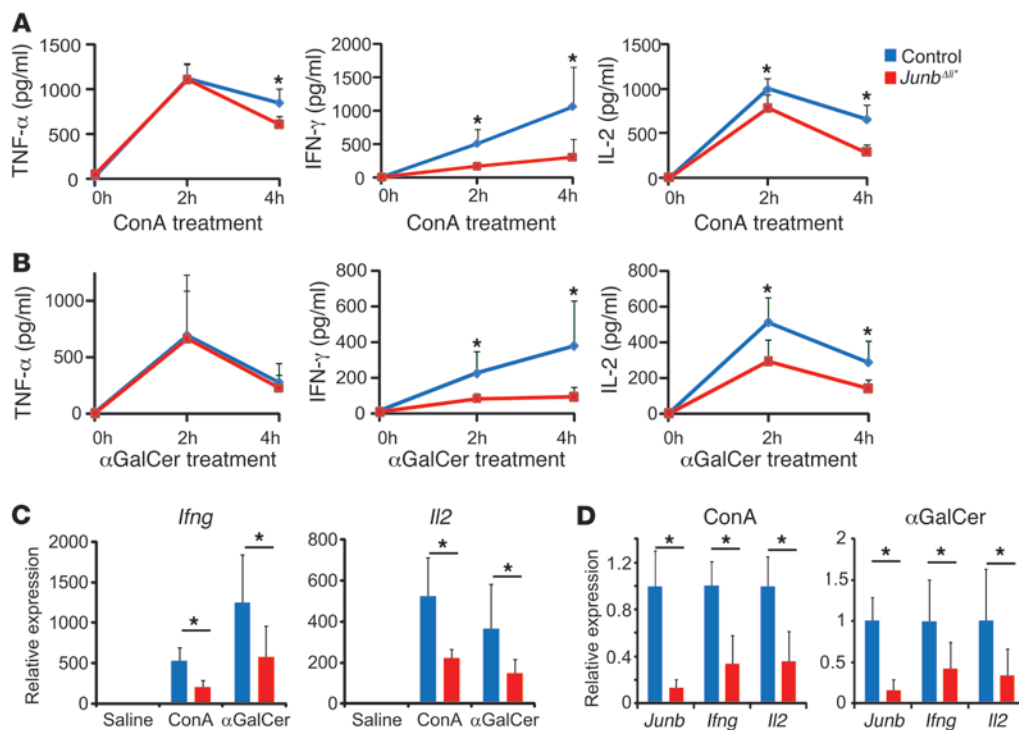
Figure 3
Junb$^{\Delta li*}$ mice have decreased cytokine levels. (**A**) Serum cytokines in control and *Junb*$^{\Delta li*}$ mice at 0 (*n* = 3), 2 (*n* = 5), or 4 (*n* = 5) hours after ConA treatment. *P < 0.05. (**B**) Serum cytokines in control and *Junb*$^{\Delta li*}$ mice at 0 (*n* = 3), 2 (*n* = 6), or 4 (*n* = 6) hours after αGalCer treatment. *P < 0.05. (**C**) qRT-PCR for *Ifng* and *Il2* in livers of control and *Junb*$^{\Delta li*}$ mice 2 hours after ConA or αGalCer treatment (*n* = 5; *P < 0.05). (**D**) qRT-PCR for *Junb*, *Ifng*, and *Il2* in spleens of control and *Junb*$^{\Delta li*}$ mice 2 hours after ConA or αGalCer treatment (*n* = 5; *P < 0.05).

mice (*Junb*$^{fl/fl}$;*AlfpCre*$^{T/+}$ mice) which lack JUNB specifically in liver parenchymal cells, but retain JUNB expression in immune cells upon ConA treatment (Supplemental Figure 2A). Importantly, serum ALT was modestly increased in *Junb*$^{\Delta li}$ mice upon ConA treatment (Supplemental Figure 2B), while no changes in *Hmox1*, *Gadd45b*, *A20*, and *Nos2* mRNA expression could be detected (Supplemental Figure 2C). This suggests that the decreased damage in *Junb*$^{\Delta li*}$ mutants is due to the loss of JUNB expression in immune cells, which is dominant over a possible hepatoprotective function of JUNB in liver parenchymal cells.

To dissect the cellular and molecular mechanisms affected by JUNB, *Junb*$^{\Delta li*}$ mice were next treated with LPS/GalN, poly-I/C, or αGalCer. LPS/GalN–induced hepatitis mainly involves TNF-α and Kupffer cells/macrophages (31) through activation of TLR4. Poly-I/C, a synthetic TLR3 ligand, mimics viral infection-associated dsRNA and elicits a cytokine response with a strong NK cell involvement (32, 33). αGalCer is proposed to cause liver injury primarily by activating NKT cells (34–36). Interestingly, while LPS/GalN injection led to comparable increase in serum ALT in *Junb*$^{\Delta li*}$ mice and control littermates (Figure 2E), a significant decrease in serum ALT was measured in *Junb*$^{\Delta li*}$ mice after αGalCer or poly-I/C administration (Figure 2F). Furthermore, poly-I/C–injected *Junb*$^{\Delta li*}$ mice had decreased levels of serum amylase and urea (Supplemental Figure 3), indicating that the protective role of JUNB deletion extends to other organs that are sensitive to IFN-γ, such as the kidney and pancreas (37). Taken together, these results indicate that loss of JUNB in immune cells is specifically protective in experimental models of hepatitis involving NK and NKT cells.

IFN-γ and IL-2 are decreased in Junb-deficient mice during hepatitis. Cytokines previously associated with each experimental model were measured in the sera of *Junb*$^{\Delta li*}$ mice. While serum TNF-α was decreased at 4 hours after ConA treatment in mutants as compared with that in control mice, it was unaffected in the other models (Figure 3, A and B, and Supplemental Figure 4C), indicating that loss of JUNB does not significantly affect TNF-α production. This finding is also consistent with comparable liver damage observed in the LPS/GalN model, a paradigm for TNF-α–mediated acute liver failure (31). Interestingly, IFN-γ and IL-2 were significantly decreased in the sera of ConA-treated *Junb*$^{\Delta li*}$ mice (Figure 3A). A similar decrease in serum IFN-γ was observed in the 2 other experimental models where JUNB deletion is protective, i.e., in αGalCer-treated (Figure 3B) and poly-I/C–treated mice (Supplemental Figure 4A) but not in LPS/GalN-treated mice (Supplemental Figure 4A). Furthermore, *Junb*$^{\Delta li*}$ mice displayed a 2-fold reduction in *Ifng* and *Il2* mRNA in the liver and the spleen 2 hours after ConA or αGalCer administration (Figure 3, C and D), indicating that decreased *Ifng* and *Il2* transcription occurs in immune cells. IL-2 was unchanged in the 2 other experimental paradigms (Supplemental Figure 4B). Other cytokines, such as IL-4, IL-6, IL-10, or IL-12p40, were comparably induced in control and mutant *Junb*$^{\Delta li*}$ mice after ConA or αGalCer treatment (Supplemental Figure 5), and loss of JUNB did not alter type I IFN induction after poly-I/C or ConA treatment (Supplemental Figure 4, D and E). Interestingly, serum IL-2 was modestly decreased in c-JUN–deficient mice (*c-Jun*$^{\Delta li*}$ or *c-Jun*$^{fl/fl}$;*MxCre*$^{T/+}$ mice) after ConA administration, while IFN-γ was unchanged (Supplemental
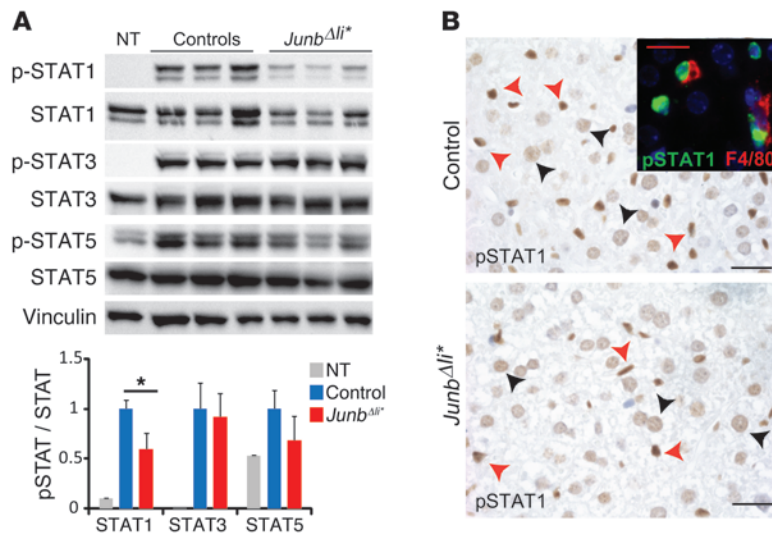
Figure 4
STAT1 pathway is altered in *Junb*^Δli*^ mice. Control and *Junb*^Δli*^ mice were treated with ConA and liver samples analyzed. (**A**) Western blot for phosphorylated and total STAT1, STAT3, STAT5. Vinculin is included to control for equal loading. Quantification is shown ($n = 5$; *$P < 0.05$). (**B**) Liver sections stained for pSTAT1 (brown) after ConA treatment. Arrowheads indicate positive immune cells (red) and hepatocytes (black). $n = 5$. Immunofluorescence costaining of pSTAT1 (green) and F4/80 (red) is shown in the inset. A representative experiment is shown. Scale bar: 20 μm.

Figure 6A). Collectively, these results indicate that reduced IFN-γ and possibly IL-2 production by immune cells might mediate the protective effect of JUNB deletion in the ConA, αGalCer, and poly-I/C experimental paradigms.

The STAT1 pathway is specifically altered in Junb-deficient mice. The STAT1 and STAT5 pathways are activated by IFN-γ and IL-2, respectively (38, 39). Phosphorylated STAT1 (pSTAT1) was decreased in liver extracts from ConA-treated *Junb*^Δli*^ mice (Figure 4A), while it was unchanged in ConA-treated *Junb*^Δli^ mice, which lack JUNB in parenchymal cells (Supplemental Figure 6B). Despite reduced IL-2 in ConA-treated *Junb*^Δli*^ mice, pSTAT5 was not significantly altered (Figure 4A). STAT3 phosphorylation was also unaffected, consistent with unchanged levels of IL-6 (Figure 4A, Supplemental Figure 5, and ref. 40). IHC analyses indicated that both hepatocytes and immune cells, which included F4/80-positive Kupffer cells, displayed nuclear pSTAT1 staining upon ConA treatment. The staining in *Junb*^Δli*^ mice seemed reduced when compared with that in control mice (Figure 4B), while no staining was observed in samples from untreated mice (data not shown).

Transcriptional targets of STAT proteins were analyzed next. *Junb*^Δli*^ mice displayed decreased mRNA expression of *Irf1*, the main target of STAT1 downstream of IFN-γ, while *Socs1*, which is regulated both by STAT1 and STAT3, was unchanged together with the bona fide STAT3 targets *Socs3* and *Bcl2l1* (refs. 36, 40, 41, and Figure 5A). Consistent with decreased IFN-γ levels, a similar impaired activation of STAT1 and *Irf1* was observed in *Junb*^Δli*^ livers in the αGalCer model (Supplemental Figure 7, A and C). IHC analyses indicated that IRF1 was induced in hepatocytes and nonparenchymal cells after ConA (Figure 5B) and αGalCer treatment (Supplemental Figure 7B). Furthermore, the number of IRF1-positive cells appeared reduced in *Junb*^Δli*^ livers (Figure 5B and Supplemental Figure 7B), and the decrease was confirmed by Western blot (Figure 5C). Importantly, IRF1 levels were unaffected in ConA-treated *Junb*^Δli^ mice (Supplemental Figure 6C).

During hepatitis, IFN-γ and activation of the STAT1 pathway are associated with hepatocyte death. STAT1 modulates *Cxcl9*, *Cxcl10*, and *Nos2* expression in hepatocytes and immune cells, and IRF1 mediates further *Nos2* induction (36, 42–44). Consistent with decreased IFN-γ, pSTAT1, and IRF1, mRNA expression of *Nos2* and *Cxcl9* was decreased in *Junb*^Δli*^ livers after ConA or αGalCer

treatment and *Cxcl10* was additionally decreased upon αGalCer treatment (Figure 5D and Supplemental Figure 7C). IHC analysis indicated that inducible NOS (iNos) was mostly expressed in immune cells, including macrophages (Supplemental Figure 8A), 2 hours after ConA treatment, as previously reported (45). Interestingly, the number of iNos-positive cells appeared reduced in *Junb*^Δli*^ livers (Supplemental Figure 8B). As the number of immune cells was unchanged in *Junb*-deficient livers after ConA treatment (Supplemental Figure 1C), this indicates that, in the absence of JUNB, iNos expression is decreased in a subset of immune cells. Moreover, dot blot analyses revealed a significant decrease in nitrosylated proteins, a readout for iNos activity, in *Junb*^Δli*^ livers 8 hours after ConA (Figure 5E).

All together, these data demonstrate that, during acute hepatitis, *Junb*^Δli*^ mice, but not *Junb*^Δli^ mice, have decreased IFN-γ/pSTAT1 pathway activity in hepatocytes and immune cells, which is likely responsible for decreased hepatotoxicity.

Decreased IFN-γ expression in NK and NKT cells lacking JUNB. T, NK, and NKT cells are the main producers of IFN-γ, with NK and NKT cells being particularly relevant in the ConA or αGalCer hepatitis paradigms (31, 36). As the number of immune cells in the liver after ConA treatment appeared unaffected by JUNB deletion, cytokine expression was analyzed in the different immune cells. Flow cytometry measurements using immune cells isolated from the liver and the spleen after in vivo ConA treatment indicated reduced intracellular IFN-γ in NK and NKT cells and decreased IL-2 in T cells isolated from *Junb*^Δli*^ mice when compared with control littermates (Supplemental Figure 9).

Next, T, NK, and NKT cells were isolated from the spleens of ConA- or αGalCer-treated *Junb*^Δli*^ mice using FACS. Molecular analyses revealed a 2-fold decrease in the expression of *Ifng* in *Junb*-deficient NK and NKT cells but not in T cells (Figure 6, A and B). On the other hand, *Il2* was decreased in *Junb*-deficient T cells, while it was undetectable in NK and NKT cells (Figure 6, A and B). These data indicate that during acute hepatitis, JUNB controls *Ifng* expression, specifically in NK and NKT cells, while it modulates *Il2* expression in T cells.

JUNB binds to the IFN-γ promoter in vivo and in vitro. We next assessed whether JUNB directly controls IFNG using ChIP assays. The mouse and human proximal *IFNG* promoter harbors a con-
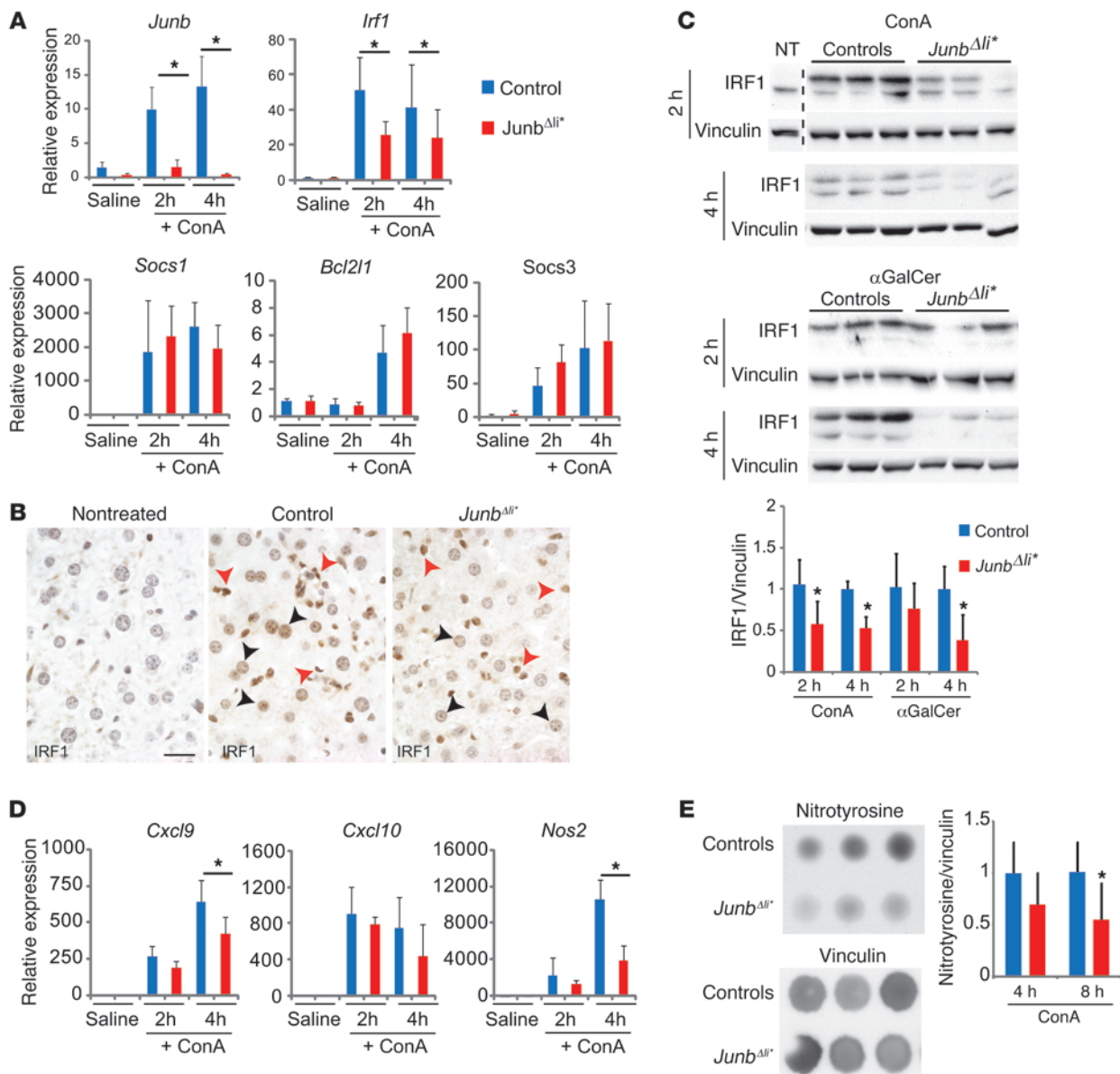
Figure 5

STAT1 targets, IRF1 and iNos, are altered in *Junb*^Δli*^ mice. Control and *Junb*^Δli*^ mice were treated with ConA or αGalCer, and liver samples were analyzed. (**A**) qRT-PCR for *Junb* and STAT-regulated genes in the livers of saline-injected mice (*n* = 3) and in mice at 2 (*n* = 5) and 4 (*n* = 5) hours after ConA. *$P < 0.05$. (**B**) Liver sections stained for IRF1 (brown) in nontreated wild-type mice or 4 hours after ConA treatment of control and *Junb*^Δli*^ mice. Arrowheads indicate positive immune cells (red) and hepatocytes (black). *n* = 3. A representative experiment is shown. Scale bar: 20 μm. (**C**) Western blot for IRF1 at 2 and 4 hours after treatment with either with ConA or αGalCer (aGal). The dotted line marks cropped samples. Vinculin is included to control for equal loading. Quantification is shown (*n* = 5–7; *$P < 0.05$). (**D**) qRT-PCR for *Cxcl9*, *Cxcl10*, and *Nos2* in the livers of saline-injected mice (*n* = 3) and in mice at 2 (*n* = 5) and 4 (*n* = 5) hours after ConA treatment. *$P < 0.05$. (**E**) Dot blot for nitrosylated proteins (nitrotyrosine) 8 hours after ConA treatment. Vinculin is included to control for equal loading. Quantification is shown (*n* = 5; *$P < 0.05$).

served TRE element (Figure 6C). ChIP analyses using whole liver extracts demonstrated that JUNB bound the chromatin region containing the TRE element in control livers but not in samples from *Junb*^Δli*^ mice (Figure 6D). No enrichment was observed when using control immunoglobulins (IgG) or when analyzing *Il2* or the ribosomal protein *S16* promoters (Figure 6D). The YT human NK cell line, which produces IFN-γ, was used next. JUNB and *IFNG* were readily detectable in basal conditions, and treatment with

PMA and ionomycin (P/I) further induced JUNB and *IFNG* expression. Low *IL2* transcript levels were also measured under these conditions (Figure 6, E and F). JUNB efficiently bound to the proximal promoter of *IFNG* in basal conditions, and increased binding was observed after P/I stimulation, while no significant binding to the *IL2* promoter was detected (Figure 6, G and H). This indicates that JUNB controls IFN-γ expression in vivo and in a human NK cell line through direct promoter binding.
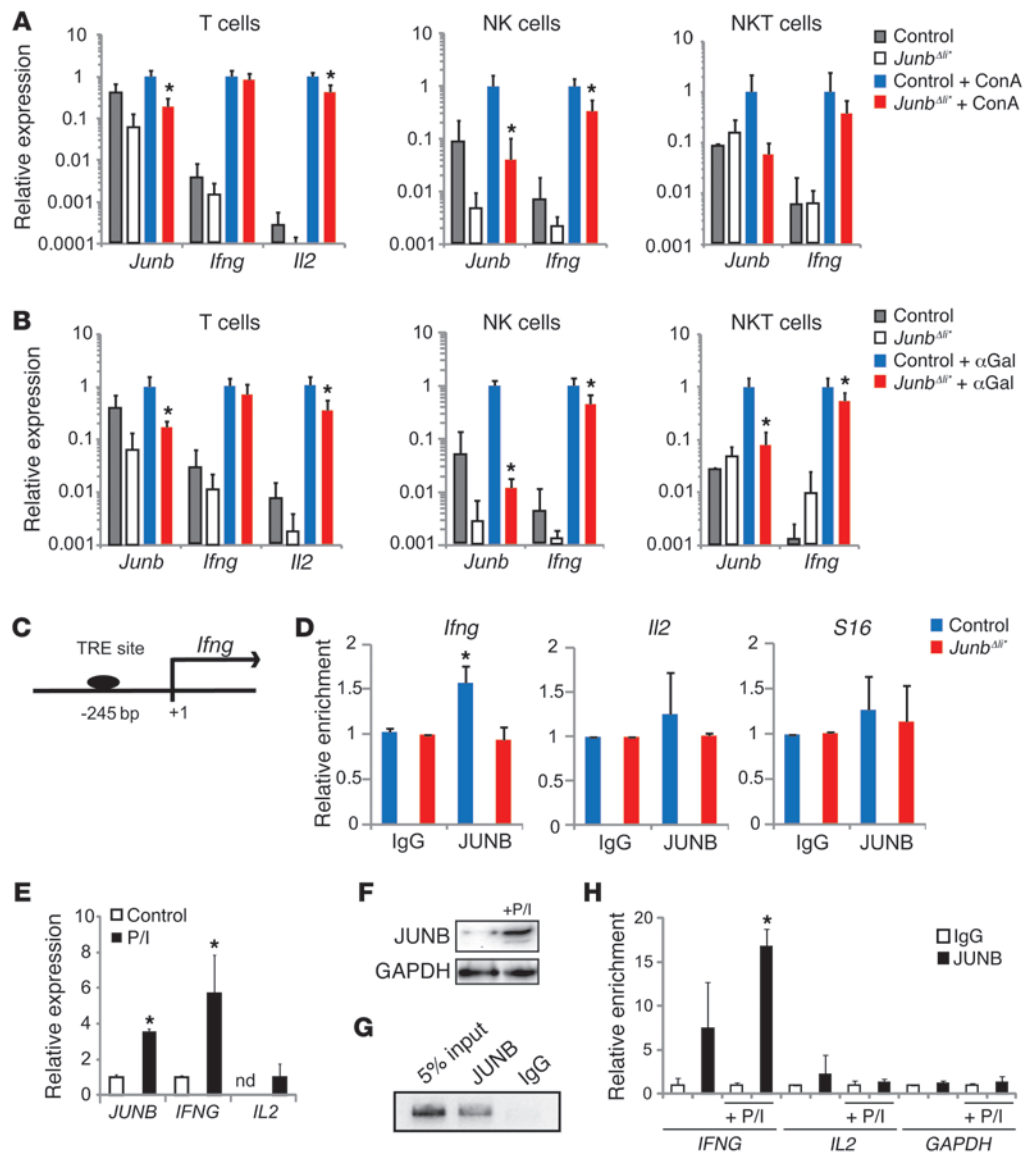
Figure 6
JUNB regulates IFN-γ in NK and NKT cells. Control and *Junb^Δli** mice were treated with (**A**) ConA or (**B**) αGalCer (*n* = 5) or not treated (*n* = 3) for 2 hours, and T (CD3+, NK1.1−), NK (CD3−, NK1.1+), and NKT (CD3+, NK1.1+) cells were isolated from spleens by flow cytometry and analyzed by qRT-PCR for gene expression. *P < 0.05. (**C**) The human/mouse *Ifng* promoter. The position of the putative AP-1 binding TRE element included in the ChIP amplicon is indicated relative to the transcription start site. (**D**) Quantitative ChIP analysis of the *Ifng*, *Il2*, and *S16* promoters in control and *Junb^Δli** livers after treatment with ConA using an antibody to JUNB or IgG. Input chromatin samples were run in parallel, and percentage of amplification relative to input for each antibody was quantified by qPCR and plotted (*n* = 3; *P < 0.05). Human YT NK cells were treated with P/I for 2 hours. (**E**) qRT-PCR expression of *JUNB*, *IFNG*, and *IL2* (*n* = 3; *P < 0.05). (**F**) Western blot analysis of JUNB. (**G**) Representative agarose gel picture of end point PCR amplification for a ChIP of the *IFNG* promoter using an antibody to JUNB or IgG in YT cells. Input chromatin sample was run in parallel. (**H**) Quantitative ChIP analysis of the *IFNG*, *IL2*, and *GAPDH* promoters in untreated or P/I-stimulated YT cells using an antibody to JUNB or IgG. Input chromatin samples were run in parallel, and the percentage of amplification relative to input for each antibody was quantified by qPCR and plotted (*n* = 3; *P < 0.05).

Restoring the pSTAT1 pathway dampens the effects of JUNB loss. To address whether alterations in the IFN-γ/STAT1/IRF1 pathway are the main contributor to decreased hepatocyte death in *Junb^Δli** mice, we treated *Junb*-deficient mice with recombinant IFN-γ. The timing and amount of IFN-γ were adjusted to achieve a level of pSTAT1 upon ConA treatment comparable to that in wild-type treated mice (Figure 7A). IFN-γ treatment did not lead to signifi-

cant liver damage in either genotype when used alone (Figure 7B). Importantly, IFN-γ restored ConA-induced liver damage in *Junb*-deficient mice to levels comparable to those of wild-type mice, as assessed by serum ALT (Figure 7B) or by analysis of stress-induced markers (Figure 7C). Furthermore, liver damage was also restored by adenovirus-based expression of *IRF1* in livers of JUNB mutant mice prior to ConA treatment (Figure 7D). These data indicate
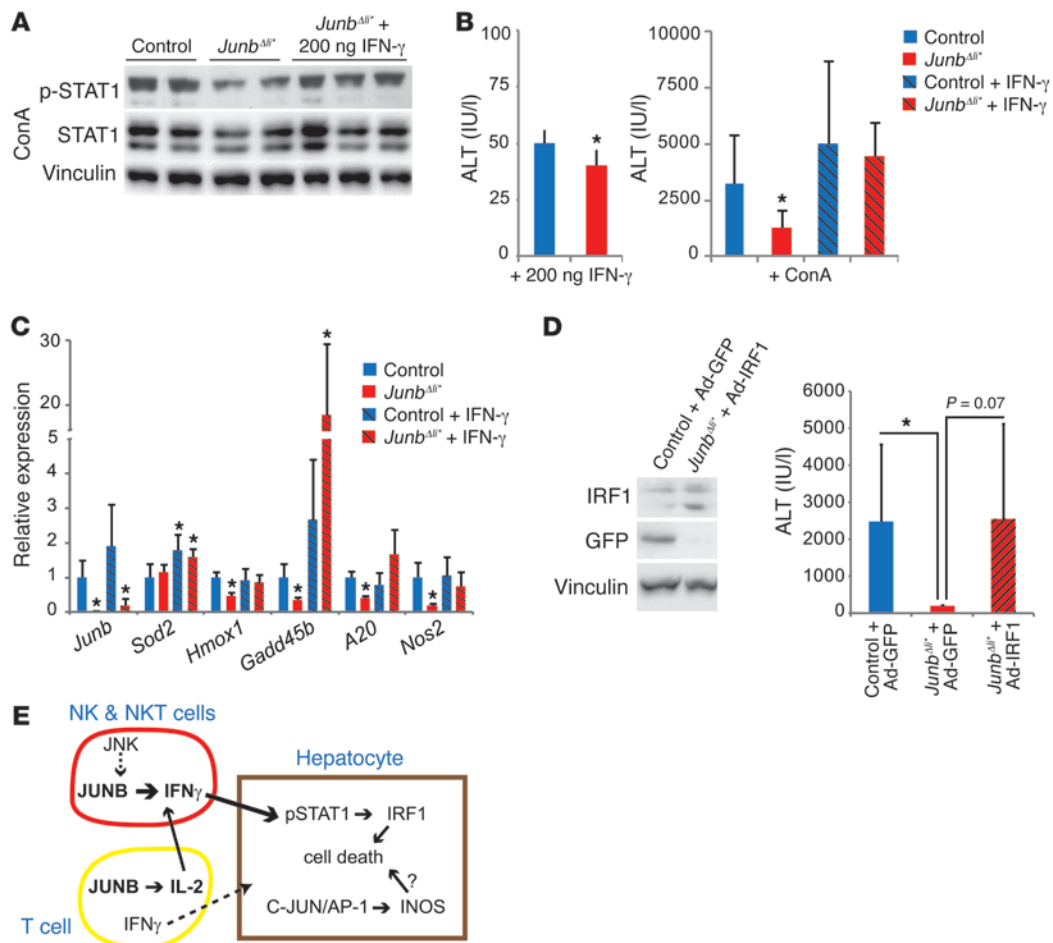
Figure 7
Restoring the IFN-γ/pSTAT1/IRF1 pathway increases liver damage. (**A**) Western blot for pSTAT1 and total STAT1 2 hours after treatment with ConA. One set of *Junb*^{Δli*} mice received 200 ng recombinant IFN-γ 1 hour after ConA treatment ($n = 3$). (**B**) Serum ALT levels 8 hours after mock or ConA injection. Left panel: control and *Junb*^{Δli*} mice received 200 ng recombinant IFN-γ 1 hour after mock treatment ($n = 3$). Right panel: all mice were treated with ConA, and a subset of control and *Junb*^{Δli*} mice received 200 ng recombinant IFN-γ 1 hour later ($n = 8$ control, $n = 5$ *Junb*^{Δli*}, 5 control plus IFN-γ, and *Junb*^{Δli*} plus IFN-γ; *$P < 0.05$). (**C**) qRT-PCR for stress-related genes in the liver 8 hours after ConA treatment. A subset of control and *Junb*^{Δli*} mice received 200 ng recombinant IFN-γ 1 hour later ($n = 4$; *$P < 0.05$, significantly different from ConA-treated control mice). (**D**) Mice were treated with adenovirus 4 days prior to ConA treatment, as indicated. Western blot for IRF1 and GFP. Vinculin is included to control for equal loading. ALT measurement 8 hours after ConA treatment ($n = 10$ control plus Ad-GFP, 3 *Junb*^{Δli*} plus Ad-GFP, 6 *Junb*^{Δli*} plus Ad-IRF1 mice; *$P < 0.05$). (**E**) Illustration of the function of JUNB in modulating acute liver injury. During acute hepatitis, JUNB regulates *Ifng* expression in NK and NKT cells and *Il2* in T cells. IL-2 increases NK and NKT cell activation. NK cell– and NKT cell–derived IFN-γ induces phosphorylation of STAT1 and the expression of STAT1 targets in hepatocytes, leading to cell death.

that decreased IFN-γ production in *Junb*-deficient immune cells during acute hepatitis and subsequent decreased STAT1/IRF1 signaling are largely responsible for decreased liver damage.

In conclusion, our data demonstrate that IFN-γ production in NK and NKT cells and IL-2 production in T cells are regulated by JUNB/AP-1 during experimental hepatitis and unravel a novel function of JUNB as an important modulator of IFN-γ hepatotoxicity in vivo (Figure 7E).

Discussion

Mouse models are instrumental in advancing our understanding of the basic mechanisms of liver homeostasis and disease (1). Here, we show a selective increase in JUNB expression in immune cells in the livers of patients with hepatitis. By combining mouse genetics

with established experimental models of liver inflammation, we have unraveled a novel function of JUNB/AP-1 in regulating IFN-γ expression in NK and NKT cells during acute hepatitis, which could potentially benefit the development of new therapies.

In mouse models, loss of JUNB decreases IFN-γ production upon ConA, poly-I/C, and αGalCer treatment but not upon LPS/GalN treatment. Consistent with impaired levels of IFN-γ, reduced active STAT1, decreased *Irf1* and *Nos2* expression, and attenuated hepatocyte death was observed. We provide evidence that *Ifng* expression is specifically decreased in NK and NKT cells lacking JUNB but not in T cells, likely due to direct and specific transcriptional regulation of *Ifng* by JUNB/AP-1 in these cells (Figure 7E). Interestingly, we found that *Ifng* was induced in T cells in response to ConA and αGalCer treatment, indicating that naive T cells might contribute to the

acute inflammatory response, similar to what has been reported in the context of *Burkholderia pseudomallei* infection (46).

We also observed that JUNB deletion leads to decreased IL-2 production in T cells from ConA- or αGalCer-treated mice, consistent with in vitro experiments demonstrating that AP-1 modulates IL-2 transcription in T cells (18, 19, 47). IL-2 triggers NK cell proliferation and activation (48) and increases IFN-γ expression in T cells (49) and NK cells (48). Therefore, decreased circulating IL-2 in *Junb^{Δli*}* mice could contribute to decreased IFN-γ production and reduced liver damage. Our data suggest that the contribution of IL-2 is likely marginal, as NK cell numbers in the liver were comparable between control and *Junb*-deficient mice and IFN-γ was unaffected in c-JUN–deficient mice, despite a reduction in circulating IL-2.

Strikingly, the function of JUNB appears both overlapping and distinct from the hepatoprotective role of its close homolog c-JUN. Hepatocytes lacking c-JUN are more prone to cell death (25, 50), and mice lacking JUNB in hepatocytes specifically also display a mild increase in ConA-induced liver damage. However, additional deletion of JUNB, but not c-JUN, in resident and circulating immune cells protects hepatocytes against ConA-induced death, indicating that the role of JUNB in immune cells is dominant over its function in hepatocytes. Interestingly, the third member of the JUN family, JUND is also important for TNF-α–induced liver damage (21, 51), but the cell-specific function of JUND has not been addressed. These studies show that JUN proteins are important for the survival of hepatocytes, although the underlying mechanisms are likely cell-context and stress-signal specific.

Nos2 is rapidly upregulated in macrophages followed by hepatocytes during acute hepatitis, leading to increased NO production. The function of *Nos2* is complex, as NO has been shown to have both cytoprotective and cytotoxic effects in the liver (52). We and others have shown that c-JUN/AP-1 regulates *Nos2* expression (25, 53, 54), and impaired *Nos2* induction upon ConA treatment in hepatocytes lacking c-JUN correlated with decreased NO and increased hypoxia, oxidative stress, and liver damage (25). Our data indicate that the function of JUNB/AP-1 during acute hepatitis is distinct from c-JUN and mediated, at least in part, by IFN-γ/pSTAT1-triggered *Nos2* induction in immune cells of the liver. In addition, mice with genetic loss of IRF1 are protected from acute inflammation (36), and our adenoviral gene-delivery experiment indicates that decreased IFN-γ/pSTAT1-triggered *Irf1* induction in *Junb*-deficient livers is likely the major contributor to the phenotype.

Besides *Nos2* and *Irf1*, IFN-γ/pSTAT1 induces *Cxcl9* and *Cxcl10* expression in macrophages (42, 43), and mice deficient for *Cxcr3*, the Cxcl9/10 receptor, display more severe ConA-induced liver injury (55). Therefore, the induction of cell death by IFN-γ/pSTAT1 in hepatocytes is counteracted by upregulation of protective chemokines by the same pathway in immune cells. Consistent with attenuated IFN-γ/pSTAT1 signaling, *Cxcl9*, and to a lesser extent *Cxcl10*, were decreased in *Junb*-deficient livers. Further work will address whether this decrease occurs specifically in macrophages and whether a direct transcriptional control of *Cxcl9/10* by AP-1 proteins contributes to decreased chemokine production.

While JNK activity has been shown to be an essential mediator of ConA-mediated liver injury (31), c-JUN is likely not a crucial target downstream of JNK in this model (25). Furthermore, experiments using JNK1 conditional alleles indicated that JNK activity is specifically required in hematopoietic cells but not in hepatocytes for the development of hepatitis and that loss of JNK in immune cells results in a marked reduction of cytokines produced by NKT cells,

including IFN-γ (56). As JUNB can be phosphorylated and activated by JNK in immune cells (20), our data imply that JUNB, rather than c-JUN, might be the relevant target downstream of JNK in immune cells modulating IFN-γ expression during acute hepatitis.

Hepatitis viruses have evolved to suppress the IFN antiviral response (57), and impaired IFN signaling is a common immune defect in human cancer (58). This might explain the rather limited benefit of IFN-based therapies in the clinic (14). However, recent data indicate that NK and NKT cells are part of the immune suppressive tumor microenvironment (59, 60) and that T cell–derived IFN-γ and TNF-α efficiently induce tumor arrest and senescence (61), prompting interest in exploring innovative cancer therapies based on the manipulation of T, NK, or NKT cells. Since a better understanding of the functions of NK and NKT cells is crucial for their rational use in tumor immunotherapies, our findings could well be relevant for cancer research.

Methods

Human samples. Hepatitis samples had Metavir scores of A1 or A2 (necroinflammatory) and between F0 and F2 (fibrosis index).

Mice and treatments. *Junb^{fl/fl}*, *MxCre*, and *AlfpCre* mice were backcrossed to C57BL/6 for a minimum of 5 generations. Four-week-old control and mutant *Junb^{Δli*}* mice were injected intraperitoneally with 13 mg/kg poly-I/C twice, with a 5-day interval, to delete the JUNB floxed allele. All subsequent experiments were carried out using 8-week-old animals. 12.5 mg/kg or 25 mg/kg ConA (Sigma-Aldrich) was injected intravenously. 30 mg/kg poly-I/C was injected intraperitoneally. 35 μg + 0.1 g/kg LPS/GalN (Sigma-Aldrich) was injected intraperitoneally. αGalCer (Funakoshi) was dissolved in 1% DMSO/PBS and delivered either intravenously or intraperitoneally at 100 μg/kg. The analysis time points, which are different between experimental models, correspond to the commonly used time points in the field. Recombinant murine IFN-γ (Tebu-Bio) was dissolved in 0.1% BSA/PBS and injected intraperitoneally. 3×10^8 PFUs of either Ad-IRF1 (SignaGen) or Ad-GFP (Iowa University) adenoviruses were injected intravenously 4 days prior to ConA treatment.

Cell culture. The human YT NK cell line was kept in RPMI with 10% FCS. Cells were left untreated or treated with 1 μM PMA and 0.5 μM ionomycin for 2 hours before processing for further analysis.

Immunohistochemistry. Tissues were fixed in 4% PFA and embedded in either paraffin or OCT. H&E staining was performed according to standard procedures. For paraffin-embedded sections, antigen retrieval was performed with a pressure cooker using citrate buffer, pH 6. The following antibodies were used for IHC: JUNB (CS3753, Cell Signaling Technology Inc.), CD68 (KP1, Dako), F4/80 (catalogue no. 123101; Biolegend), pSTAT1 (CS9171, Cell Signaling Technology Inc.), and IRF1 (SC-640, Santa Cruz Biotechnology Inc.), together with matching secondary antibodies coupled with a fluorescent dye (Invitrogen) or using the VECTA-STAIN Elite ABC Kits (Vector Laboratories). iNos (catalog no. 610332, BD Biosciences) staining was performed on frozen sections, and secondary anti-rabbit coupled to AF594 or HRP was used. Counterstaining was performed with DAPI or hematoxylin.

Flow cytometry and cell sorting. Immune cells were isolated from the spleen or the liver 2 hours after treatment with either ConA or αGalCer. The whole organ was pressed through a 70-μm (spleen) or 100-μm (liver) cell strainer. Liver immune cells were further isolated by 38% to 70% Percoll gradient centrifugation. Red blood cells were lysed (R7757, Sigma-Aldrich). Cells were next incubated with FC-Block (BD) and the following antibodies against immune cell surface markers: F4/80 (Biolegend) and CD3, CD4, CD8, and NK1.1 (all from BD Bioscience). For JUNB intracellular staining, cells were next fixed in 2% PFA, permeabilized with

0.1% Triton X-100, and incubated with primary (anti-JUNB, CS3753) and secondary (anti-rabbit AF594, Invitrogen) antibody. For IFN-γ and IL-2 intercellular staining, single cells were treated with Golgi Stop (BD) but not restimulated. Cells were stained with cell surface markers and then fixed and permeabilized with BD Bioscience fixation and permeabilization buffers. Data were acquired on a BD LSRII Fortessa and analyzed using FlowJo 9.5.3. At least 5,000 individual living cells were collected. The different immune cell populations were gated as follows: T cells: CD3⁺, NK1.1⁻; NK cells: CD3⁻, NK1.1⁺; NKT cells: CD3⁺, NK1.1⁺; CD4⁺ T cells: CD4⁺, CD8⁻; CD8⁺ T cells: CD4⁻, CD8⁺; and macrophages and monocytes: F4/80⁺. For RNA isolation, splenocytes were stained with CD3 and NK1.1 antibodies, and single-positive (T or NK) cells and double-positive (NKT) cells were sorted using a BD INFLUX sorter.

Blood analyses. Blood was collected by heart puncture. Serum parameters were measured using a VetScan Chemistry Analyzer (Abaxis) or a Reflovet Plus blood chemistry analyzer (Scil Diagnostics) according to the manufacturer's instructions. Serum cytokines were measured using the CBA Flex Set Cytometric Bead Array (BD Bioscience) for IL-2, IL-4, IL-6, IL-10, IL-12p40, IFN-γ, TNF-α, and Cxcl9 and the ELISA Kit for IFN-β (VeriKine).

Protein isolation, Western blot, and dot blot. Tissues were disrupted using a Precellys 24 device (Bertin Technologies) in RIPA buffer containing a protease inhibitor cocktail (Sigma-Aldrich), 0.1 mM Na_3VO_4, 40 mM B-glycerophosphate, 40 mM NaPPi, and 1 mM NaF. For Western blot analysis, 50 μg protein per sample was loaded, and membranes were blocked with 2.5% BSA in TBS-T before incubation with primary antibody. The following antibodies were used: pSTAT1 (CS9171, Cell Signaling Technology Inc.), pSTAT3 (CS3131, Cell Signaling Technology Inc.), pSTAT5 (CS9351, Cell Signaling Technology Inc.), STAT1 (SC-346, Santa Cruz Biotechnology Inc.), STAT3 (CS9132, Cell Signaling Technology Inc.), STAT5 (SC-835, Santa Cruz Biotechnology Inc.), cleaved caspase-3 (CS9661, Cell Signaling Technology Inc.), IRF1 (SC-640, Santa Cruz Biotechnology Inc.), and GFP (ab290-50, abcam) For dot blots, 15 μg protein was spotted on a PVDF membrane and blocked with 5% milk in TBS-T before incubation with anti-Nitrotyrosine antibody (06-284, Millipore). HRP-linked secondary antibodies were purchased from Amersham and DAKO.

qRT-PCR. RNA was isolated with TRIzol (Sigma-Aldrich) and complementary DNA synthesized with Ready-To-Go-You-Prime-First-Strand Beads (GE Healthcare), using 1 μg DNAse-pretreated total RNA and random hexamers. Quantitative PCR was performed using GoTaq qPCR Master Mix (Promega) and an Eppendorf fluorescence thermocycler. The com-

parative cycle threshold method was used for quantification. Expression levels were normalized using at least one housekeeping gene (*Actb*, *Gapdh*). See Supplemental Table 1 for primer sequences.

ChIP. ChIP was performed as previously described (25). Chromatin was immunoprecipitated using JUNB antibody (CS3753) or IgG (Millipore). qPCR was used to monitor amplified fragments.

Statistics. All experiments were performed at least 3 times, and data in bar graphs represent mean ± SD of the indicated sample numbers. For ALT measurement, randomized block design was applied to account for variation among litters. Statistical analysis was performed using nondirectional 2-tailed Student's *t* test, except for analysis of Kaplan-Meier curves, for which a log-rank (Mantel-Cox) test was used. *P* < 0.05 was considered as significant.

Study approval. Paraffin sections of needle biopsies from healthy patients and patients with chronic hepatitis were provided by the CNIO tumor bank in accordance with the ethical guidelines of the Helsinki Declaration. Mouse handling and experimentation was done in accordance with and with the approval of local and institutional guidelines and regulations (the ethics commission for animal research and welfare under Institución Carlos III).

Address correspondence to: Erwin F. Wagner, Genes, Development and Disease Group, National Cancer Research Centre (CNIO), F-BBVA Cancer Cell Biology Programme, Melchor Fernandez Almagro 3, 28029 Madrid, Spain. Phone: 34.91.224.69.12; Fax: 34.91.224.69.14; E-mail: ewagner@cnio.es.

1. Bakiri L, Wagner EF. Mouse models for liver cancer. *Mol Oncol.* 2013;7(2):206–223.
2. Herkel J, Schuchmann M, Tiegs G, Lohse AW. Immune-mediated liver injury. *J Hepatol.* 2005; 42(6):920–923.
3. Stauffer JK, Scarzello AJ, Jiang Q, Wiltrout RH. Chronic inflammation, immune escape, and oncogenesis in the liver: a unique neighborhood for novel intersections. *Hepatology.* 2012;56(4):1567–1574.
4. El-Serag HB, Rudolph KL. Hepatocellular carcinoma: epidemiology and molecular carcinogenesis. *Gastroenterology.* 2007;132(7):2557–2576.
5. Rehermann B, Nascimbeni M. Immunology of hepatitis B virus and hepatitis C virus infection. *Nat Rev Immunol.* 2005;5(3):215–229.
6. Borden EC, et al. Interferons at age 50: past, current and future impact on biomedicine. *Nat Rev Drug Discov.* 2007;6(12):975–990.
7. Zhang SY, et al. Inborn errors of interferon (IFN)-mediated immunity in humans: insights into the respective roles of IFN-α/β, IFN-γ, and IFN-λ in host defense. *Immunol Rev.* 2008;226:29–40.
8. George PM, Badiger R, Alazawi W, Foster GR, Mitchell JA. Pharmacology and therapeutic potential of interferons. *Pharmacol Ther.* 2012;135(1):44–53.
9. Agnello D, et al. Cytokines and transcription factors that regulate T helper cell differentiation: new players and new insights. *J Clin Immunol.* 2003;23(3):147–161.
10. Schoenborn JR, Wilson CB. Regulation of interferon-γ during innate and adaptive immune responses. *Adv Immunol.* 2007;96:41–101.
11. Kakimi K, Guidotti LG, Koezuka Y, Chisari FV. Natural killer T cell activation inhibits hepatitis B virus replication in vivo. *J Exp Med.* 2000;192(7):921–930.
12. Zeissig S, et al. Hepatitis B virus–induced lipid alterations contribute to natural killer T cell–dependent protective immunity. *Nat Med.* 2012;18(7):1060–1068.
13. Ishikawa T. Immunoregulation of hepatitis B virus infection — rationale and clinical application. *Nagoya J Med Sci.* 2012;74(3–4):217–232.
14. Horras CJ, Lamb CL, Mitchell KA. Regulation of hepatocyte fate by interferon-gamma. *Cytokine Growth Factor Rev.* 2011;22(1):35–43.
15. Eferl R, Wagner EF. AP-1: a double-edged sword in tumorigenesis. *Nat Rev Cancer.* 2003;3(11):859–868.
16. Wagner EF, Eferl R. Fos/AP-1 proteins in bone and the immune system. *Immunol Rev.* 2005;208:126–140.
17. Cippitelli M, et al. Negative transcriptional regulation of the interferon-gamma promoter by glucocorticoids and dominant negative mutants of c-Jun. *J Biol Chem.* 1995;270(21):12548–12556.
18. Rincon M, Flavell RA. AP-1 transcriptional activity requires both T-cell receptor-mediated and co-stimulatory signals in primary T lymphocytes. *EMBO J.* 1994;13(18):4370–4381.
19. Wisniewska MB, Ameyar-Zazoua M, Bakiri L, Kaminska B, Yaniv M, Weitzman JB. Dimer composition and promoter context contribute to functional cooperation between AP-1 and NFAT. *J Mol Biol.* 2007;371(3):569–576.
20. Li B, Tournier C, Davis RJ, Flavell RA. Regulation of IL-4 expression by the transcription factor JunB during T helper cell differentiation. *EMBO J.* 1999; 18(2):420–432.
21. Meixner A, Karreth F, Kenner L, Wagner EF. JunD regulates lymphocyte proliferation and T helper cell cytokine expression. *EMBO J.* 2004;23(6):1325–1335.
22. Guinea-Viniegra J, et al. TNFα shedding and epidermal inflammation are controlled by Jun proteins. *Genes Dev.* 2009;23(22):2663–2674.
23. Meixner A, et al. Epidermal JunB represses G-CSF transcription and affects haematopoiesis and bone formation. *Nat Cell Biol.* 2008;10(8):1003–1011.
24. Passegue E, Jochum W, Behrens A, Ricci R, Wagner EF. JunB can substitute for Jun in mouse devel-

opment and cell proliferation. *Nat Genet.* 2002; 30(2):158–166.

25. Hasselblatt P, Rath M, Komnenovic V, Zatloukal K, Wagner EF. Hepatocyte survival in acute hepatitis is due to c-Jun/AP-1-dependent expression of inducible nitric oxide synthase. *Proc Natl Acad Sci U S A.* 2007;104(43):17105–17110.

26. Tiegs G, Hentschel J, Wendel A. A T cell-dependent experimental liver injury in mice inducible by concanavalin A. *J Clin Invest.* 1992;90(1):196–203.

27. Schumann J, et al. Importance of Kupffer cells for T-cell-dependent liver injury in mice. *Am J Pathol.* 2000;157(5):1671–1683.

28. Matsuoka S, et al. A monoclonal antibody to the alpha2 domain of murine major histocompatibility complex class I that specifically kills activated lymphocytes and blocks liver damage in the concanavalin A hepatitis model. *J Exp Med.* 2003; 198(3):497–503.

29. Nakashima H, et al. Superoxide produced by Kupffer cells is an essential effector in concanavalin A-induced hepatitis in mice. *Hepatology.* 2008;48(6):1979–1988.

30. Takeda K, Hayakawa Y, Van Kaer L, Matsuda H, Yagita H, Okumura K. Critical contribution of liver natural killer T cells to a murine model of hepatitis. *Proc Natl Acad Sci U S A.* 2000;97(10):5498–5503.

31. Maeda S, Chang L, Li ZW, Luo JL, Leffert H, Karin M. IKKbeta is required for prevention of apoptosis mediated by cell-bound but not by circulating TNFalpha. *Immunity.* 2003;19(5):725–737.

32. Alexopoulou L, Holt AC, Medzhitov R, Flavell RA. Recognition of double-stranded RNA and activation of NF-κB by Toll-like receptor 3. *Nature.* 2001; 413(6857):732–738.

33. Zhang M, et al. The β2 integrin CD11b attenuates polyinosinic:polycytidylic acid-induced hepatitis by negatively regulating natural killer cell functions. *Hepatology.* 2009;50(5):1606–1616.

34. Shimosaka A. Role of NKT cells and alpha-galactosyl ceramide. *Int J Hematol.* 2002;76(suppl 1):277–279.

35. Biburger M, Tiegs G. α-Galactosylceramide-induced liver injury in mice is mediated by TNF-α but independent of Kupffer cells. *J Immunol.* 2005; 175(3):1540–1550.

36. Cao Z, Dhupar R, Cai C, Li P, Billiar TR, Geller DA.

A critical role for IFN regulatory factor 1 in NKT cell-mediated liver injury induced by α-galactosyl-ceramide. *J Immunol.* 2010;185(4):2536–2543.

37. Hayashi T, Ishida Y, Kimura A, Iwakura Y, Mukaida N, Kondo T. IFN-γ protects cerulein-induced acute pancreatitis by repressing NF-κB activation. *J Immunol.* 2007;178(11):7385–7394.

38. Hou J, Schindler U, Henzel WJ, Wong SC, Mc Knight SL. Identification and purification of human Stat proteins activated in response to interleukin-2. *Immunity.* 1995;2(4):321–329.

39. Shuai K, Schindler C, Prezioso VR, Darnell JE. Activation of transcription by IFN-gamma: tyrosine phosphorylation of a 91-kD DNA binding protein. *Science.* 1992;258(5089):1808–1812.

40. Klein C, et al. The IL-6-gp130-STAT3 pathway in hepatocytes triggers liver protection in T cell-mediated liver injury. *J Clin Invest.* 2005;115(4):860–869.

41. Naka T, et al. SOCS-1/SSI-1-deficient NKT cells participate in severe hepatitis through dysregulated cross-talk inhibition of IFN-γ and IL-4 signaling in vivo. *Immunity.* 2001;14(5):535–545.

42. Ohmori Y, Hamilton TA. Requirement for STAT1 in LPS-induced gene expression in macrophages. *J Leukoc Biol.* 2001;69(4):598–604.

43. Hiroi M, Ohmori Y. The transcriptional coactivator CREB-binding protein cooperates with STAT1 and NF-κB for synergistic transcriptional activation of the CXC ligand 9/monokine induced by interferon-γ gene. *J Biol Chem.* 2003;278(1):651–660.

44. Tsuge M, et al. Hepatitis C virus infection suppresses the interferon response in the liver of the human hepatocyte chimeric mouse. *PLoS One.* 2011;6(8):e23856.

45. Schumann J, Prockl J, Kiemer AK, Vollmar AM, Bang R, Tiegs G. Silibinin protects mice from T cell-dependent liver injury. *J Hepatol.* 2003;39(3):333–340.

46. Koo GC, Gan YH. The innate interferon gamma response of BALB/c and C57BL/6 mice to in vitro Burkholderia pseudomallei infection. *BMC Immunol.* 2006;7:19.

47. Garaude J, et al. SUMOylation regulates the transcriptional activity of JunB in T lymphocytes. *J Immunol.* 2008;180(9):5983–5990.

48. Biron CA, Young HA, Kasaian MT. Interleukin 2-induced proliferation of murine natural killer

cells in vivo. *J Exp Med.* 1990;171(1):173–188.

49. Shi M, Lin TH, Appell KC, Berg LJ. Janus-kinase-3-dependent signals induce chromatin remodeling at the Ifng locus during T helper 1 cell differentiation. *Immunity.* 2008;28(6):763–773.

50. Eferl R, et al. Liver tumor development. c-Jun antagonizes the proapoptotic activity of p53. *Cell.* 2003;112(2):181–192.

51. Weitzman JB, Fiette L, Matsuo K, Yaniv M. JunD protects cells from p53-dependent senescence and apoptosis. *Mol Cell.* 2000;6(5):1109–1119.

52. Chen T, Zamora R, Zuckerbraun B, Billiar TR. Role of nitric oxide in liver injury. *Curr Mol Med.* 2003; 3(6):519–526.

53. Xu W, et al. STAT-1 and c-Fos interaction in nitric oxide synthase-2 gene activation. *Am J Physiol Lung Cell Mol Physiol.* 2003;285(1):L137–L148.

54. Gough DJ, et al. A novel c-Jun-dependent signal transduction pathway necessary for the transcriptional activation of interferon γ response genes. *J Biol Chem.* 2007;282(2):938–946.

55. Erhardt A, et al. CXCR3 deficiency exacerbates liver disease and abrogates tolerance in a mouse model of immune-mediated hepatitis. *J Immunol.* 2011; 186(9):5284–5293.

56. Das M, Sabio G, Jiang F, Rincon M, Flavell RA, Davis RJ. Induction of hepatitis by JNK-mediated expression of TNF-α. *Cell.* 2009;136(2):249–260.

57. Gale MJ, et al. Evidence that hepatitis C virus resistance to interferon is mediated through repression of the PKR protein kinase by the nonstructural 5A protein. *Virology.* 1997;230(2):217–227.

58. Critchley-Thorne RJ, et al. Impaired interferon signaling is a common immune defect in human cancer. *Proc Natl Acad Sci U S A.* 2009;106(22):9010–9015.

59. Lindau D, Gielen P, Kroesen M, Wesseling P, Adema GJ. The immunosuppressive tumour network: myeloid-derived suppressor cells, regulatory T cells and natural killer T cells. *Immunology.* 2013; 138(2):105–115.

60. Vivier E, Ugolini S, Blaise D, Chabannon C, Brossay L. Targeting natural killer cells and natural killer T cells in cancer. *Nat Rev Immunol.* 2012;12(4):239–252.

61. Braumuller H, et al. T-helper-1-cell cytokines drive cancer into senescence. *Nature.* 2013; 494(7437):361–365.